Applied Physics A (2026) 132:728
https://doi.org/10.1007/s00339-026-09923-2

Applied Physics A
Materials Science & Processing

Enrichment of specific capacitance and functional properties of Polytetrafluoroethylene composite work with CNT/graphene hybrids

Ruba M.[1] · Navuluri Padma Sravya[2] · Ganesh Murali J.[3] · S. Selvam[4] · C. Gnanavel[5] · S. Prabagaran[6] · R. Srinivasan[7] · M. Ramya[8] · S. Sathiyamurthy[9] · Anand Rajendran[10]

Received: 16 March 2026 / Accepted: 6 July 2026

Abstract

Polytetrafluoroethylene (PTFE) is widely used in high-frequency electronic applications due to its unique properties, including superior chemical resistance, dielectric properties, and thermal stability. This material is integrated into the electrode system to have better energy storage. However, it found low electrical conductivity, reduced sheet resistance, and variations in surface area limit the functional properties of PTFE. This research aims to enhance the functional properties of PTFE by embedding it with different ratios of carbon nanotube (CNT)-graphene hybrids via a vacuum filtration production method. The influences of CNT-graphene hybrids on sheet resistance, conductivity, BET surface area, thickness, areal loading, Raman (ID/IG ratio), and specific capacitance (F/G) of PTFE are investigated and related to the base (PTFE matrix). The 30:70 CNT: Graphene hybrid composition exhibited optimal performance, with a sheet resistance of 145 Ω/sq and an electrical conductivity of 158 S/m. The Brunauer–Emmett–Teller (BET) surface area, thickness, and areal loading were measured to be 1163 m²/g, 16 μm, and 1.20 mg/cm². The Raman ratio was 0.96 for the 30:70 compositions, and the specific capacitance was 292 F/g. This composition of PTFE/CNT/graphene hybrid is a trade-off for electrode applications.

Keywords Carbon nanotube · Electrode application · Graphene · Properties · Production · Polytetrafluoroethylene

✉ M. Ramya
ramyamaranan451@gmail.com

Ruba M.
rubamcse@krce.ac.in

Navuluri Padma Sravya
sravyapadma4@gmail.com

Ganesh Murali J.
ganeshmurali.j@kce.ac.in

S. Selvam
cuddaloreselvam@gmail.com

C. Gnanavel
gnanavelmech1986@gmail.com

S. Prabagaran
s.prabagaran.cbe@gmail.com

R. Srinivasan
srinivasansimats@gmail.com

S. Sathiyamurthy
ssathya1978@gmail.com

Anand Rajendran
dranandrajendran@yahoo.com

[1] Department of Computer Science and Engineering, K. Ramakrishnan College of Engineering, Trichy, Tamil Nadu 621112, India

[2] Department of Mechanical Engineering, Geethanjali Institute of Science and Technology, Nellore, Andhra Pradesh 524137, India

[3] Department of Mechanical Engineering, Karpagam College of Engineering, Coimbatore, Tamilnadu 641032, India

[4] Department of Aeronautical Engineering, Nehru Institute of Engineering and Technology, Coimbatore, Tamil Nadu 641105, India

[5] Department of Mechanical Engineering, Vels Institute of Science, Technology and Advanced Studies, Pallavaram, Chennai, Tamil Nadu 600117, India

[6] Department of Mechanical Engineering, Karpagam Academy of Higher Education, Coimbatore, Tamil Nadu 641021, India

[7] Department of Mechanical Engineering, Saveetha School of Engineering, Saveetha Institute of Medical and Technical Sciences, SIMATS, Chennai, Tamil Nadu 602105, India

[8] Division of Research and Development, Lovely Professional University, Jalandhar - Delhi G.T. Road, Phagwara, Punjab 144411, India

[9] Jerusalem College of Engineering, Pallikaranai, Chennai, Tamil Nadu 600100, India

[10] Lloyd Institute of Engineering & Technology, Plot No. 3, Knowledge Park II, Greater Noida, Uttar Pradesh 201306, India

Published online: 13 July 2026

Nomenclature

A	Coated electrode area (cm^2)
I	Applied current (A), Discharge current (A)
m	Mass of the active material (g)
n	Number of scan points
t	Film thickness (cm)
V	Measured potential difference (V), molar volume of nitrogen (cm^3g^{-1})
σ	Electrical conductivity (S/cm), Molecular cross-sectional area of nitrogen (nm^2)
Δt	Discharge time (s)
ΔV	Potential window (V)

Subscripts

C_{sp}	Specific capacitance (F/g)
h_i	Measured height of the deposited film at point i (nm)
h_0	Baseline substrate height (nm)
I_D	Intensity of D band (cm^{-1})
I_G	Intensity of G band (cm^{-1})
M_f	Total mass (mg)
M_s	Mass of bare substrate (mg)
N_A	Avogadro's number
R_s	Sheet resistance (Ω/sq)
S_{BET}	Brunauer–Emmett–Teller surface area (m^2/g)
V_m	Monolayer capacity (cm^3g^{-1})

Abbreviations

BET	Brunauer–Emmett–Teller
CNT	Carbon NanoTube
PTFE	Polytetrafluoroethylene
PVA	PolyVinyl Alcohol
UV	Ultra-Violet

1 Introduction

PTFE is a highly adaptable material recognized for its promising properties, which have led to its extensive use in membrane-based separation, purification, biomedical, and energy-related fields. Recent research has focused on improving PTFE membrane fabrication techniques, refining pore structure management, and enhancing functionalization to address existing limitations and broaden the scope of PTFE membranes in a wide range of applications [1]. PTFE also provided exceptional chemical resistance and hydrophobicity. However, its processing introduced challenges for conventional and 3D printing techniques. A study presented a UV-based 3D micro-printing methodology for creating pure PTFE microstructures. This widened its application in super-hydrophobic surfaces and sophisticated micro/nano-engineering fields [2]. Electron irradiation of PTFE has been shown to improve its microhardness, wear resistance, and tribological properties. Thus, it enhanced its mechanical robustness; however, this might cause deterioration in its thermal properties. This suggested a need to analyze the balance between mechanical performance and potential thermal degradation in irradiation-modified PTFE [3]. The chemical inert nature of PTFE led to minimal wettability and low adhesion in certain devices. This can be improved through plasma treatment, which can modify the surface from hydrophobic to hydrophilic, primarily via UV-induced bond modification [4].

Additionally, treatment with ammonia water–assisted plasma jet significantly improved the PTFE surface hydrophilicity and adhesive strength, outperforming both untreated surfaces and those treated with helium plasma alone [5]. Additionally, PTFE exhibited minimal friction and corrosion resistance in aqueous lubrication systems. But its wear resistance is limited, leading to the addition of ceramic particles into PTFE. For seawater lubrication, silicon carbide and hexagonal boron nitride (h-BN) fillers have demonstrated superior wear resistance [6]. The ability of the PTFE film to reversibly transform between hydrophobic and hydrophilic states could facilitate dynamic dual functionality in applications such as light modulation, anti-fogging, and thermal management, thereby highlighting PTFE's considerable potential for advanced smart surface technologies [7].

Shao et al. [8] investigated a PTFE/graphene-based hydrophobic coating that demonstrated remarkable performance. The coating's superior adhesion, self-cleaning capabilities, and corrosion resistance were attributed to the influence of difluorocarbene (CF2)/ trifluoromethyl (CF3) bonds, as well as the presence of exposed nanostructures. These combined improvements position the coating as a promising material for future engineering applications. Another study investigated PTFE/CNT nanofiber membranes, which showed improved mechanical robustness, electrical conductivity, and EM wave attenuation, with very low reflection loss at a 1 wt% CNT concentration. These composite materials also retained their inherent hydrophobicity, thermal stability, and oil-absorption capacity in oil-water separation applications [9]. The graphene nano sheets/PTFE composite film demonstrated exceptional electromagnetic interference (EMI) shielding effectiveness. This composite also exhibited superior thermal conductivity, flexibility, and robustness, which can be attributed to its distinctive structural morphology. The study investigates and production of the inherent properties of heat resistance, dual nature, and recyclability, made high dependable material for large-scale industrial operation in extreme conditions [10]. Liu et al. [11] analyzed a polymer electrolyte fuel cell with the incorporation of a PTFE binder (10 wt%). The results showed significantly reduced

mass transportation and resistance. The study also revealed that a higher PTFE content increased the blockage of active sites, affecting mass transport and leading to rapid performance degradation in the electrolyte fuel cell. The utilization of cryo-pulverized PTFE as a binder in sulfide-based all-solid-state batteries has been shown to facilitate homogeneous dispersion. This resulted in a decrease in electrical resistance and an increase in ionic and electronic conductivity. This strategic enhancement yields superior capacity retention (90.4%) and robust cycling performance, rendering it suitable for dry-film electrode fabrication [12]. The synthesized fluorine (F) and nitrogen (N)-co-doped porous carbon material, production from a PTFE-based sponge precursor, exhibits a substantial surface area and superior electrochemical properties. This mesoporous carbon achieved a specific capacitance of 299 F/g.

Furthermore, its notable energy density and robust cycling stability highlighted its potential in supercapacitor applications [13]. Another study defluorinated PTFE using lithium ions, producing a porous carbon material with a BET surface area of 1045 m^2/g and an excellent specific capacitance of 199 F/g. This performance exceeded that of activated carbon fibers with comparable surface areas. The superior electrochemical properties are due to its optimized pore architecture and beneficial surface characteristics [14]. The synthesis of porous carbons via the defluorination of PTFE using potassium resulted in materials with a high specific capacitance of 229 F/g. This enhanced performance is attributed to the synergistic effect of both microporous and mesoporous structures within the carbons [15]. This highlights the importance of a porous surface morphology in the PTFE electrode. In the synthesis of PTFE with CNT: graphene hybrids, vacuum filtration is chosen among various fabrication methods because it achieves a homogeneous distribution and precise layering of nanomaterials into a dense, thin film. The vacuum pressure facilitated effective solvent extraction, enhancing interfacial bonding between PTFE and the hybrid fillers. This method yielded consistent thickness and surface loading, simultaneously improving conductivity and mechanical integrity for use in lightweight electrodes [16, 17].

However, the closely related past literature on Polytetrafluoroethylene (PTFE) is elaborated above, and it was found that PTFE processed with monolithic filler via conventional methods exhibits low electrical conductivity, variations in BET surface area, and reduced sheet resistance, which limit the overall performance of the PTFE structure. The main objectives of the present research are to synthesize the PTFE structure by integrating different ratios of CNT: graphene layers via vacuum filtration and to enhance the electrical conductivity, sheet resistance, and BET surface area of the PTFE structure. Furthermore, this study investigates the effect of the CNT/graphene ratio on sheet resistance, conductivity, BET surface area, thickness, areal loading, Raman (ID/IG ratio), and specific capacitance (F/G) of PTFE, and it relates these outcomes to the base PTFE matrix without CNT/graphene hybrids.

2 Materials and methods

2.1 Materials selection

PTFE powder (30–50 nm) was selected for its exceptional chemical inertness, thermal resilience, and low density [2], making it a valuable base polymer matrix in this study. Graphene nanoplatelets (5 µm lateral size and 50 nm thickness) were added as the conductive filler, providing substantial surface area to the composite. The substance is manufactured and supplied by Ad-Nano Technologies, which was received from the MS Research and Development Department, Saveetha University, Chennai, Tamil Nadu, India. It has enhanced electron mobility and provided active sites for electrochemical reactions [7]. To improve mechanical robustness and conductive pathways, CNTs (2 µm in length) were incorporated into the composite as high-aspect-ratio reinforcements [9]. Otto Chemie Pvt. Ltd. manufactured CNT fibre from the MS. Research and Development Department, Saveetha University, Chennai, Tamil Nadu, India. Deionized water served as the dispersion medium, selected for its high purity, ready availability, and compatibility with ultrasonication-assisted mixing, thereby avoiding contamination.

Trace quantities of ammonium hydroxide (NH_4OH, 25 wt%) were introduced to function as a surfactant, thereby enhancing the colloidal stability of CNTs and graphene in aqueous medium. Polyvinyl alcohol (PVA) is used in a minimal quantity as a temporary binder to enhance film quality in the filtration process before post-treatment [17]. PTFE-supported membranes served as the base substrate for filtration, promoting homogeneous deposition and facilitating easy peeling of the composite films. The basic behaviour of PTEF, CNT, and graphene is presented in Table 1.

2.2 Fabrication procedure

PTFE composite films, reinforced with a combination of CNT and graphene hybrids, were successfully manufactured via a vacuum filtration method, as demonstrated in Fig. 1. Table 2 presents the optimal fabrication process parameters [16, 17]. Table 3 shows the composition details for PTEF film fabrication with CNT and graphene.

The study used PTFE powder (0.45 µm) as the base material, incorporating CNT and graphene nanoplatelets

Table 1 Properties table of PTFE, CNT, and graphene

Property	PTFE	CNT	Graphene	Ref
Electrical conductivity (S/m)	$\sim 10^{-25}$	$\sim 10^{3}$-10^{5}	$\sim 10^{6}$	[7, 18]
Electrical resistivity (Ω.cm)	$\sim 10^{23}$	10^{-4}-10^{-6}	10^{-6}	[7, 9]
Thermal conductivity (W/m.K)	0.25	3000	2000–5000	[7, 9]
Tensile strength	25 MPa	50–200 GPa	130 GPa	[7, 9]

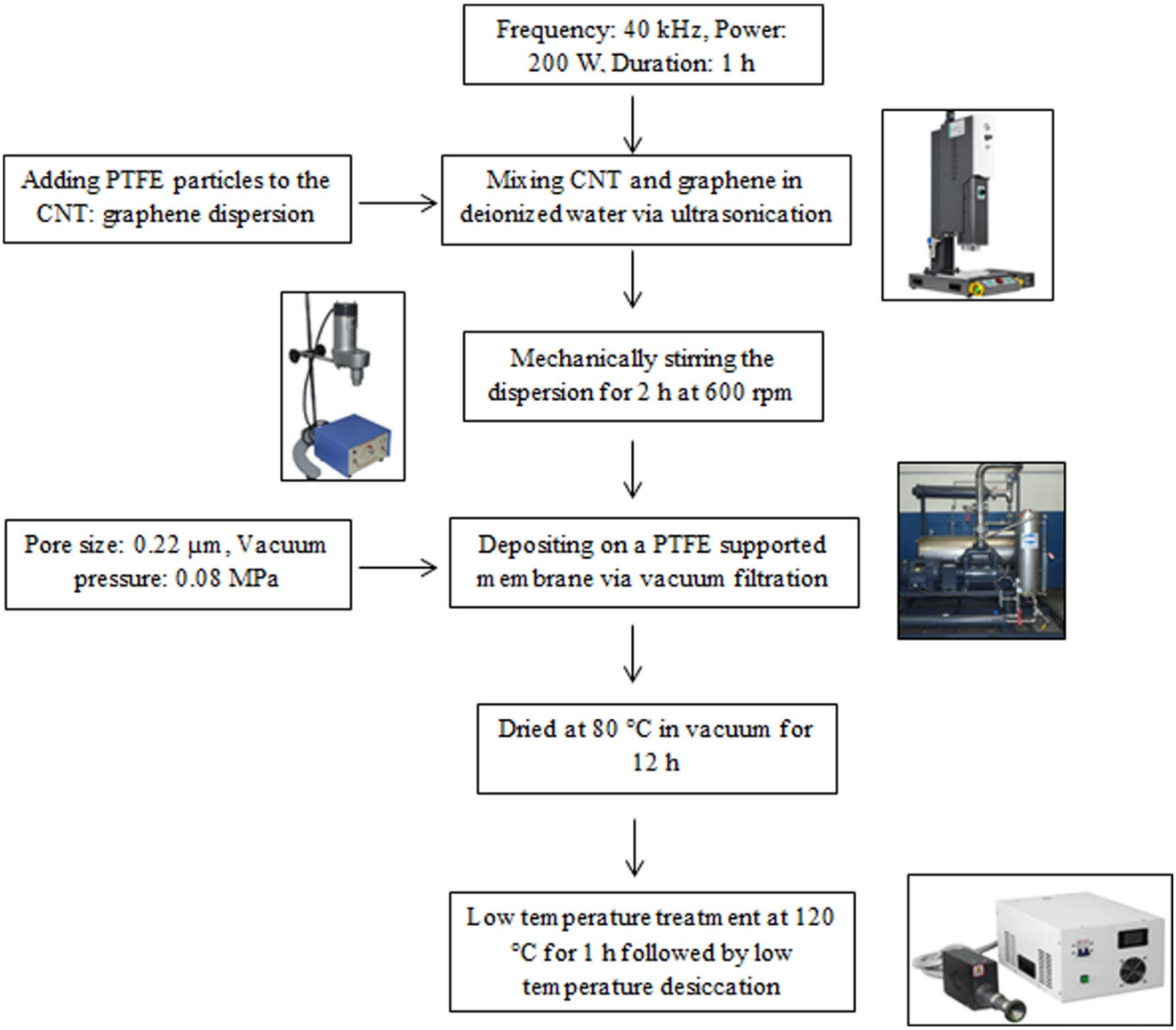

Fig. 1 Sequential fabrication steps of PTFE hybrid composites

to enhance conductivity. The study explored four distinct ratios of the CNT: graphene hybrid (10:90, 20:80, 30:70, 40:60), with a pristine PTFE sample serving as a baseline for evaluation.

To ensure a homogeneous mixture and prevent particle aggregation, the CNT and graphene components were initially suspended in deionized water using ultrasonication at 40 kHz and 200 W for 1 h. Subsequently, PTFE particles were added to this dispersion, maintaining a 1:1 ratio of polymer to hybrid material. The mixture was then mechanically stirred at 600 rpm for 2 h, followed by a final 30-minute ultrasonication cycle to achieve a uniform dispersion of the nanofillers [16, 19].

The resulting suspensions were deposited by vacuum filtration through a PTFE-supported membrane with a pore size of 0.22 µm, under a vacuum pressure of 0.08 MPa to

Table 2 Fabrication parameters

Step	Parameter	Condition
CNT: graphene dispersion	Concentration	0.5 mg/mL in deionized water
	Ultrasonication	40 kHz, 200 W, 1 h
PTFE mixing	Stirring	600 rpm, 2 h
	Ultrasonication	30 min
Vacuum filtration	Membrane	0.22 µm pore size
	Vacuum pressure, Time	0.08 MPa, 30 min
Drying	Vacuum oven	80 °C, 12 h
Thermal treatment	Annealing	120 °C, 1 h

Table 3 Composition details for PTEF film

Sample identification	PTEF film compositions
PTFE	PTFE
PTFE 1	PTFE with 10:90 CNT: Graphene
PTFE 2	PTFE with 20:80 CNT: Graphene
PTFE 3	PTFE with 30:70 CNT: Graphene
PTFE 4	PTFE with 40:60 CNT: Graphene

expedite solvent removal and facilitate the formation of a dense, uniform film [17]. The filtration process was carried out for 30 min, based on composition, to ensure a consistent film thickness. After deposition, the wet cakes were dried at 80 °C under vacuum for 12 h to remove any residual material. A subsequent low-temperature treatment at 120 °C for 1 h was implemented to enhance the compatibility between PTFE and CNT–graphene hybrids [10]. The synthesized composite films were detached from the filtration membrane and placed in a desiccator at 20% relative humidity prior to analysis. The unmodified PTFE and PTFE matrices incorporated with CNT: graphene hybrid materials in weight ratios of 10:90, 20:80, 30:70, and 40:60 were synthesized. These films were characterized, revealing that optimized CNT–graphene hybrids, achieved through optimized deposition conditions, yielded electrode films that were lightweight, electrically conductive, and thermally stable, making them suitable for future electrochemical applications.

2.3 Characterization

The sheet resistance, mentioned in Eq. (1) [6, 20], is practically determined using a Keithley 2400 source meter, a four-point probe measurement system, with fixed tungsten carbide tips with 1 mm probe spacing. The applied current was set to 5 mA, and profilometry was used for areal-loading corrections.

$$R_s = \frac{\pi}{\ln(2)} \frac{V}{I} \tag{1}$$

By using Eq. (2) [7], the electrical conductivity was calculated. The applied current was maintained at 1 mA with 1 mm probe spacing. The measurement was carried out in a room at ambient temperature.

$$\sigma = \frac{1}{R_s \times t} \tag{2}$$

The Brunauer–Emmett–Teller (BET) method was used to evaluate the surface area of the electrodes using Eq. (3) [13], with a Micromeritics ASAP 2020 surface area and porosity analyzer. The nitrogen gas (99.99% purity) was used as an adsorbate, and the samples were degassed at 120 °C under prior investigation. The relative pressure (P/P_0) of 0.2 was maintained in the BET fitting.

$$S_{BET} = \frac{V_m N_A \sigma}{V} \tag{3}$$

The Ambios XP-200 stylus profilometer was used to measure the electrode thickness using Eq. (4) [14]. To measure thickness, a 5 mg stylus force was used with a scan speed of 0.05 mm/s and a vertical resolution of 10 nm. Areal loading was measured using a profilometer with a precise analytical balance with a ± 0.01 mg precision. Equation (5) [14] characterizes the areal loading of the electrode with PTFE supported membrane substrate.

$$t = h_{avg} = \frac{1}{n} \sum_{i=1}^{n} (h_i - h_0) \tag{4}$$

$$Areal\ loading = \frac{M_f - M_s}{A} \tag{5}$$

The intensity ratio of the D and G bands from Raman spectroscopy was measured using a confocal micro-Raman

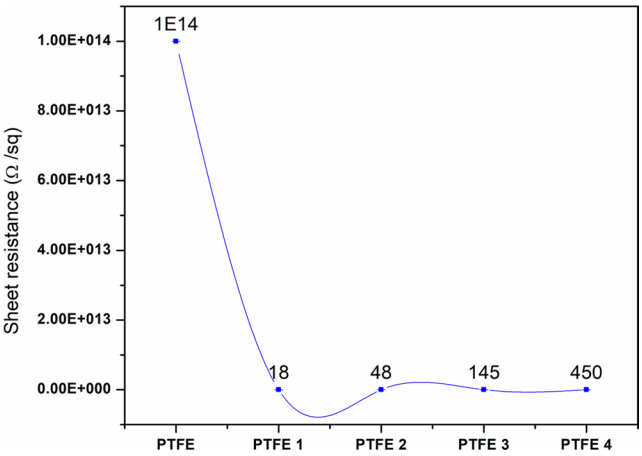

Fig. 2 Sheet resistance analysis of PTFE and CNT: graphene-loaded PTFE composites

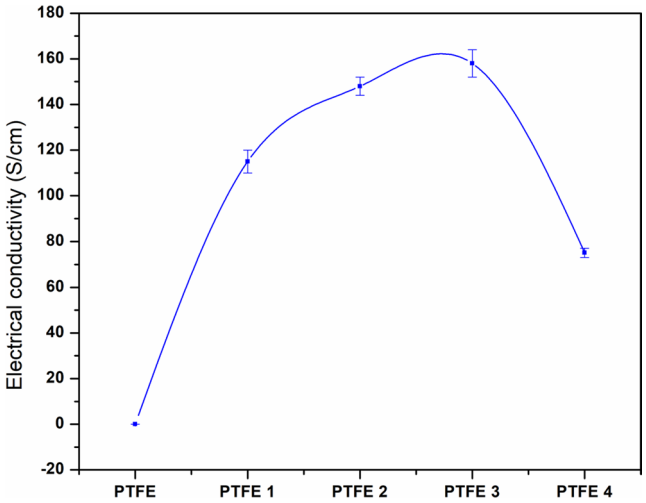

Fig. 3 Conductivity analysis of PTFE and CNT: graphene-loaded PTFE composites

spectrometer, as described in Eq. (6) [15]. A 532 nm excitation laser was used with the laser power maintained at 1 mW. Spectral evaluation was performed using a 50x objective lens and a 1 cm^{-1} spectral resolution.

$$\frac{I_D}{I_G} = \frac{Intensity\ of\ D\ band\ at\ 1350\ cm^{-1}}{Intensity\ of\ G\ band\ at\ 1580\ cm^{-1}} \tag{6}$$

The specific capacitance of the electrode was determined from the galvanostatic charge-discharge (GCD) measurements, using Eq. (7) [3]. A potentiostat-galvanostat was used in conjunction with a three-electrode electrochemical cell setup featuring a silver (Ag) reference electrode. A current density of 5 A/g was used with a potential window of 1 V. The measurement was carried out at room temperature with an active material loading of 3 mg/cm².

$$C_{sp} = \frac{I\Delta t}{m\Delta V} \tag{7}$$

3 Results and discussions

3.1 Sheet resistance

Figure 2 shows the sheet resistance (R_S) results of the fabricated pristine PTFE and PTFE composites with CNT-graphene hybrid loading. The analysis showed a significant reduction in the R_S of PTFE with higher hybrid content. The pristine PTFE sheet exhibited a high sheet resistance of approximately 10^{14} Ω/sq.

This is due to its intrinsic insulating nature and the lack of any conductive filler [3]. When PTFE was incorporated into a 10:90 CNT: graphene hybrid, the R_S was reduced to 18 Ω/sq. This significant decline in RS is attributed to charge delocalization and the conducting platform facilitated by the higher graphene content [7]. However, the minimal CNT content limited three-dimensional conduction pathways, resulting in higher RS than in other CNT-dominant compositions. With a 20:80 CNT: graphene composition, the PTFE composite showed a further marginal hike in R_S of the order 48 Ω/sq, as the CNT content ensured the formation of effective conductive bridges. This facilitated enhanced electron tunnelling and reduced the resistance between graphene nanoplatelets, demonstrating the combined influence of CNTs and graphene in enhancing electrical conductivity [10]. The PTFE with 30:70 CNT: graphene composition demonstrated the R_S, approximately 145 Ω/sq, among all the compositions. The 1D CNTs established continuous conduction pathways, while graphene contributed superior carrier mobility and interfacial conductivity, thus effectively reducing junction resistance and enhancing charge transport efficiency [9]. A slight rise in sheet resistance was observed, reaching 450 Ω/sq when the CNT content exceeded 30% in PTFE: 40:60 of CNT: Graphene hybrid. This is likely due to the agglomeration of CNTs at elevated concentrations, which impeded uniform dispersion and diminished effective connectivity with the graphene sheets. The optimal composition was found to be 30:70 CNT: graphene, which facilitates a synergistic network in which graphene enhances carrier mobility, and CNTs provide conductive pathways over longer distances.

3.2 Electrical conductivity

The electrical conductivity of PTFE-based composites is highly dependent on the ratio of CNT: graphene hybrids used for reinforcement, as shown in Fig. 3.

The pristine PTFE demonstrated a bulk conductivity of the order of 10^{-14} S/m. While PTFE is an insulator, the addition of CNT: graphene hybrids created conductive networks that significantly improved charge transport [9]. The 10:90 CNT: graphene/PTFE composite exhibited a conductivity of 115 S/m. The predominant presence of graphene contributed to high in-plane conductivity and an extensive surface area. Conversely, the limited proportion of CNTs facilitated inter-sheet bridging, thereby minimizing electron scattering. The 20:80 CNT: graphene/PTFE composite exhibited enhanced charge transport capabilities, as evidenced by a conductivity increase to 148 S/m and a corresponding reduction in sheet resistance, as mentioned in Sect. 3.1. This specific hybrid ratio establishes a more effective conductive network while preserving a substantial active surface area. The composition of 30:70 CNT: graphene/PTFE exhibited the most favourable electrical properties, characterized by peak conductivity of 158 S/m and minimal sheet resistance. This outcome is attributed to the synergistic interplay between CNTs and graphene, which effectively reduces restacking, enhances electron mobility, and promotes the development of a uniform network [7]. For the 40:60 CNT: graphene/PTFE composite, a slight decline in electrical conductivity was observed with the value of 75 S/m. Despite increased CNT concentration, excessive loading appears to reduce the effective contact area between graphene layers and to elevate junction resistance due to inter-tube interactions. Thus, the 30:70 CNT: graphene/PTFE composition exhibited optimal electrical performance, characterized by low resistance and high conductivity.

3.3 BET surface area

Figure 4 demonstrates the influence of incorporating a hybrid composition on the BET surface area of PTFE composites. The specific surface area of pristine PTFE was measured to be the lowest at 227 m^2/g. This is due to its dense nature and non-porous structural morphology [2]. The introduction of CNT–graphene hybrids significantly enhances the available surface area, as graphene offers a high surface area, and CNTs facilitate a porous structural morphology. When the CNT: graphene ratio was 10:90, the surface area of the PTFE composite experienced a significant increase to 763 m^2/g, as the dominant graphene planes offered high surface area to the composite. Further increasing the CNT content to 20% with 80% graphene increased the surface area to 981 m^2/g. This improvement is attributed to the CNTs' role as spacers, which prevented graphene sheet restacking and facilitated the formation of additional mesoporous [21]. The highest BET surface area, 1163 m2/g, was achieved with a 30:70 CNT: graphene ratio. This composition represents a promising configuration, where CNTs provide optimal structural

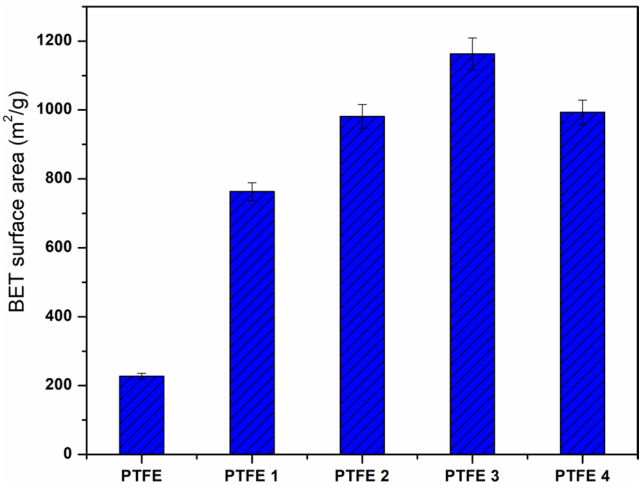

Fig. 4 BET surface area of PTFE and CNT: Graphene-loaded PTFE composites

separation and graphene provides sufficient accessibility, resulting in a well-interconnected porous structure [22].

At higher CNT concentrations, the surface area was observed to decline, reaching 993 m^2/g for a 40:60 CNT: graphene hybrid composition. This decrease is attributed to the agglomeration of CNTs and increased packaging density, which, in turn, reduces the accessibility of the graphene surfaces [23]. These results highlight the importance of optimizing the PTFE composites, with a 30:70 composition providing the highest surface area and improved electrical performance.

3.4 Thickness and areal loading

Figure 5 reveals a clear compositional ratio-dependent variation in the thickness and areal loading of the PTFE composites. The PTFE film, without any hybrid loading, exhibited a consistent thickness of 12.0 µm and an areal

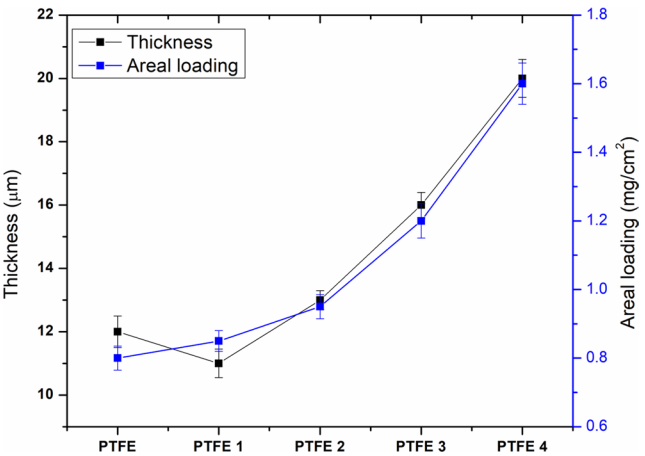

Fig. 5 Thickness and areal loading of PTFE and CNT: graphene-loaded PTFE composites

loading of 0.80 mg/cm². This uniformity is attributed to the material's dense structure and lack of conductive additives. When CNT: graphene hybrids were incorporated at a 10:90 ratio, a slight reduction in thickness to 11.0 µm was observed, accompanied by a minor increase in areal loading to 0.85 mg/cm^2. This is due to the dominant graphene's densely packed planar arrangement [7], while the small proportion of CNT minimally affects this aggregation, allowing for increased PTFE entrapment within the composite structure [21]. The 20:80 CNT: graphene ratio increased the thickness to 13.0 µm and the areal loading to 0.95 mg/cm^2. This composition facilitates improved pore formation, and the increased CNT content retained in the pores limits graphene restacking.

At a 30:70 ratio, these effects were more significant, with thicknesses reaching 16.0 µm and an areal loading of 1.20 mg/cm². The CNT network created substantial porosity, resulting in a larger cake volume relative to mass and a reduced rate of solvent permeation, which improved overall density [19, 20]. The PTFE with a 40:60 CNT: graphene composite showed the highest thickness of 20 µm and an areal loading of 1.60 mg/cm²; however, the high CNT content affects graphene stacking, leading to higher porosity and reduced gravimetric efficiency.

3.5 Raman (I_D/I_G ratio)

The structural disorder and degree of graphitization within the PTFE and CNT: graphene hybrids incorporated in PTFE composites were assessed using Raman spectroscopy, as demonstrated in Fig. 6. The PTFE composite exhibited minimal D- and G-band activity, with an ID/IG ratio of approximately 0, reflecting its non-conductive properties. This is due to the lack of sp^2-conjugated carbon domains. The incorporation of CNT-graphene hybrids revealed a clear pattern in the ID/IG ratio that correlated with increasing CNT content. For a 10:90 CNT: graphene ratio, a comparatively low I_D/I_G ratio of 0.80 was observed.

This is attributed to the high graphene content and the minimal structural defects resulting from the high degree of sp2 ordering, which improve conductivity and reduce the composite's sheet resistance [9]. The 20:80 CNT: graphene composition showed an ID/IG ratio of 0.90, indicating a marginal increase in structural disorder. This observation is attributed to the formation of tube-graphene junctions and interfacial defects [10]. An increase in CNT concentration, as observed in the PTFE with a CNT: graphene (30:70) composition, led to a higher I_D/I_G ratio of 0.96. This suggests an elevated defect density at the interface between the CNT junction and the polymer layer. While this heightened disorder was associated with reduced long-range conductivity, the creation of these defect sites concurrently improved other electrical and electrochemical properties [13]. The 40:60 composite displayed the greatest degree of disorder, with an I_D/I_G ratio of 1. This heightened disorder is attributed to disrupted hybrid composite dispersion and packing alignment, as well as increased interfacial strain between the CNTs and PTFE.

3.6 Specific capacitance

The specific capacitance of PTFE and CNT: graphene hybrid composites, prepared through vacuum filtration, is significantly influenced by the proportion of CNTs and graphene within the PTFE matrix, as mentioned in Fig. 7.

Pure PTFE displayed minimal capacitance (46 F/g), due to its insulating properties and lack of electrochemically active sites. The incorporation of CNT-graphene hybrid materials into the PTFE matrix resulted in a significant

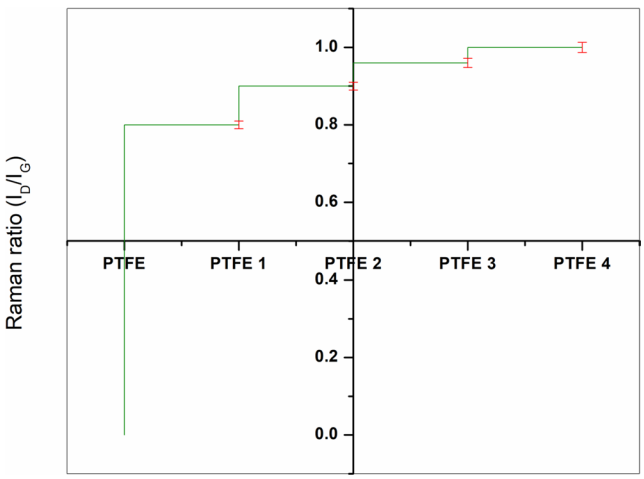

Fig. 6 Raman ratio analysis of PTFE and CNT: Graphene-loaded PTFE composites

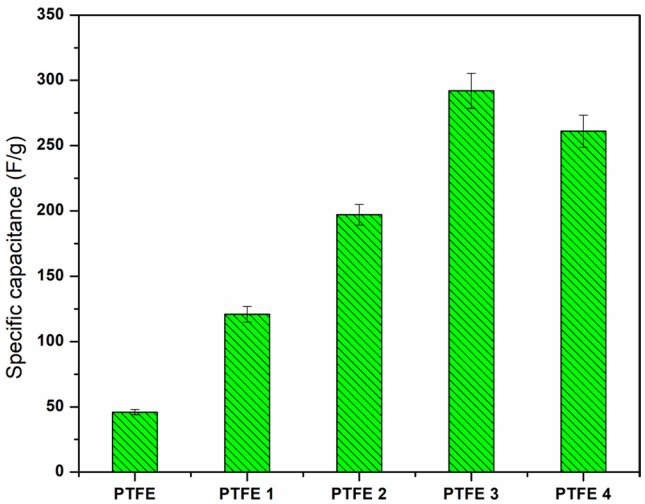

Fig. 7 Specific capacitance analysis of PTFE and CNT: graphene-loaded PTFE composites

Table 4 Comparison study of the present paper with previous papers

S. No	Compositions	BET surface area (m^2/g)	Specific capacitance (F/g)	Ref no.
1	PTFE-derived nitrogen and fluorine co-doped mesoporous carbon	1799	284	[13]
2	Defluorinated PTFE-derived porous carbon with lithium metal	1084	199	[14]
3	PTFE-derived porous carbon with potassium	999	237	[15]
4	PTFE with 30:70 CNT: graphene hybrid composition	1163	292	Present paper

improvement in capacitance. The 10:90 CNT: graphene ratio demonstrated a capacitance of 121 F/g, attributed to the substantial BET surface area provided by graphene and the conductive networks initially formed by CNTs [15]. Increasing the CNT content to 20% further enhanced the capacitance to 197 F/g, due to the reduced sheet resistance and increased effective charge transport within the polymer matrix [9]. Peak performance was observed with a PTFE composition of 30:70 CNT: graphene, yielding a maximum specific capacitance of 292 F/g. This composition achieved an optimal balance between the enhanced surface area provided by graphene and the robust conductive pathways established by CNTs. This effectively minimized resistance to ion diffusion and improved electrolyte access [13]. At a ratio of PTFE:40:60 CNT: graphene, the capacitance diminished to 261 F/g. This decrease is likely due to an excessive concentration of CNTs, which reduced the effective surface area. This reduction in surface area is caused by the agglomeration and restacking of conductive fillers, thereby limiting the number of active charge storage sites.

As shown in Table 4, the present work demonstrates significant enhancements in specific capacitance, with 2.8% improvement over nitrogen/fluorine co-doped PTFE/carbon [13], 46.7% over Li-defluorinated carbon [14], and 23.2% over K-derived PTFE/carbon [15]. The BET surface area of the present paper demonstrated 7.3% and 16.4% improvement over Li-defluorinated carbon [14] and K-derived PTFE/carbon [15], but showed 35.3% reduction compared to nitrogen/fluorine co-doped PTFE/carbon [13]. Despite having a smaller surface area than the N/F co-doped material, the current study demonstrates superior specific capacitance. This suggests that the synergistic combination of CNT and graphene enhances charge storage more effectively, making it a more suitable option for lightweight electrode applications.

4 Conclusion

This study successfully fabricated a Polytetrafluoroethylene (PTFE) composite using different ratios of carbon nanotube-graphene (CNT: graphene) hybrids via vacuum filtration. The effectiveness of CNT: graphene on the functional properties of PTFE was evaluated, and it was found that the 30:70 CNT: graphene ratio yielded better results than others. The sheet resistance, electrical conductivity, BET surface area, and thickness & areal loading of the 30:70 CNT/graphene-embedded PTFE composite are 99.9%, more than 100%, 412%, 66.7% and 100% better than the PTFE matrix without CNT/graphene. Raman spectroscopy indicated that integrating CNT: graphene hybrids led to a gradual increase in structural disorder. This result showed an approximate Raman ratio of 0.96, which is superior to that of pristine PTFE, indicating enhanced interfacial activity and an elevated overall electrochemical performance of the hybrid composite material. The hybrid composites also showed improved electrochemical performance. Specifically, the 30:70 composition exhibited a maximum of 534% enhancement in specific capacitance. This outcome highlights the synergistic effect of graphene's extensive surface area and CNT's efficient conductive networks, resulting in superior charge storage. While the study focuses on electrochemical characteristics, a comprehensive evaluation of the long-term structural integrity and mechanical resilience of PTFE–CNT-graphene composites is lacking. Future studies should investigate the tensile strength, flexibility, and fatigue resistance of flexible and wearable electrode materials. In addition, the excess CNTs led to diminished performance, highlighting challenges in filler dispersion and homogeneity. Future research should consider methods such as surfactant-assisted mixing, in situ growth, or chemical functionalization to address CNT agglomeration and enhance filler-matrix interactions.

Author contributions All the authors contributed to the study's conception and design. Material preparation, data collection and analysis were carried out by Ruba. M, Navuluri Padma Sravya, Ganesh Murali. J, S. Selvam, C. Gnanavel, S. Prabagaran, R. Srinivasan, M. Ramya, S. Sathiyamurthy, Anand Rajendran. The first manuscript draft was prepared by M. Ramya, and subsequently, all the authors contributed to the finalization of the manuscript.

Funding The authors did not receive support from any organization for the submitted work.

Data availability All the data required are available within the manuscript.

Declarations

Ethics approval This is an observational study. Enrichment of specific capacitance and functional properties of Polytetrafluoroethylene composite embedded with CNT/graphene hybrids: The Research Ethics Committee has confirmed that no ethical approval is required.

Competing & financial interests The authors have no relevant financial or non-financial interests to disclose. The authors have no competing interests to declare relevant to this article's content. All authors certify that they have no affiliations with or involvement in any organizationor entity with any financial or non-financial interest in the subject matter or materials discussed in this manuscript. The authors have no financial or proprietary interests in any material discussed in this article.

References

1. Q. Guo, Y. Huang, M. Xu, Q. Huang, J. Cheng, S. Yu, C. Xiao, PTFE porous membrane technology: a comprehensive review. *Journal of Membrane Science*. Elsevier B.V (2022, December 15). https://doi.org/10.1016/j.memsci.2022.121115
2. Y. Zhang, M.J. Yin, X. Ouyang, A.P. Zhang, H.Y. Tam, 3D μ-printing of polytetrafluoroethylene microstructures: a route to super-hydrophobic surfaces and devices. Appl. Mater. Today. 19 (2020). https://doi.org/10.1016/j.apmt.2020.100580
3. K.D. Ormanbekov, B.K. Rakhadilov, A.Z. Zhassulan, N.E. Mukhamedov, A.B. Shynarbek, N.M. Magazov, Effect of electron irradiation on mechanical, tribological and thermal properties of Polytetrafluoroethylene. Eurasian J. Phys. Funct. Mater. **7**(4), 221–231 (2023). https://doi.org/10.32523/EJPFM.2023070402
4. G. Primc, Recent advances in surface activation of Polytetrafluoroethylene (PTFE) by gaseous plasma treatments. Polymers. MDPI AG (2020, October 1). https://doi.org/10.3390/polym12102295
5. Li, Y., Zhou, Y., Gu, Y., Chen, B., Wang, B., Yan, J., Liu, X, Improving surface wettability and adhesion property of Polytetrafluoroethylene by atmospheric-pressure ammonia water-mixed plasma treatment. Vacuum. **196** (2022). https://doi.org/10.1016/j.vacuum.2021.110763
6. B. Lin, A. Wang, T. Sui, C. Wei, J. Wei, S. Yan, Friction and wear resistance of polytetrafluoroethylene-based composites reinforced with ceramic particles under aqueous environment. Surf. Topogr. Metrol. Prop. **8**(1) (2020). https://doi.org/10.1088/2051-672X/ab6e23
7. Yin, K., Wu, J., Deng, Q., Wu, Z., Wu, T., Luo, Z., Duan, J. A. Tailoring micro/nanostructured porous polytetrafluoroethylene surfaces for dual-reversible transition of wettability and transmittance. Chem. Eng. J. **434** (2022). https://doi.org/10.1016/j.cej.2022.134756
8. W. Shao, D. Liu, T. Cao, H. Cheng, J. Kuang, Y. Deng, W. Xie, Study on Favourable Comprehensive Properties of Super-hydrophobic Coating Fabricated by Polytetrafluoroethylene Doped with Graphene. Adv. Compos. Hybrid. Mater. **4**(3), 521–533 (2021). https://doi.org/10.1007/s42114-021-00243-y
9. Huang, A., Liu, F., Cui, Z., Wang, H., Song, X., Geng, L., Peng, X. Novel PTFE/CNT composite nanofiber membranes with enhanced mechanical, crystalline, conductive,and dielectric properties fabricated by emulsion electrospinning and sintering. Compos. Sci. Technol. **214** (2021). https://doi.org/10.1016/j.compscitech.2021.108980
10. Wei, Q., Li, L., Deng, Z., Wan, G., Zhang, Y., Du, C., Wang, G. Scalable fabrication of nacre-structured graphene/polytetrafluoroethylene films for outstanding EMI shielding under extreme environment. Small. **19**(35) (2023). https://doi.org/10.1002/smll.202302082
11. S. Liu, K. Wippermann, W. Lehnert, Mechanism of action of polytetrafluoroethylene binder on the performance and durability of high-temperature polymer electrolyte fuel cells. Int. J. Hydrog. Energy. **46**(27), 14687–14698 (2021). https://doi.org/10.1016/j.ijhydene.2021.01.192
12. K. Lee, Y. Jo, J. Seok Nam, H. Yu, Y.J. Kim, Dry-film technology employing cryo-pulverized polytetrafluoroethylene binder for all-solid-state batteries. Chem. Eng. J. **487** (2024). https://doi.org/10.1016/j.cej.2024.150221
13. H. Jia, J. Zhu, M. Zhang, S. Sang, F. Hu, F. Zhang, Fluorine and nitrogen co-doped mesoporous carbon derived from polytetrafluoroethylene@melamine sponge for supercapacitor application. J. Energy Storage. **38** (2021). https://doi.org/10.1016/j.est.2021.102613
14. S. Shiraishi, H. Kurihara, H. Tsubota, A. Oya, Y. Soneda, Y. Yamada, Electric double layer capacitance of highly porous carbon derived from lithium metal and Polytetrafluoroethylene. Electrochem. Solid-State Lett. **4**(1) (2001). https://doi.org/10.1149/1.1344276
15. Y. Yamada, O. Tanaike, T.T. Liang, H. Hatori, S. Shiraishi, A. Oya, Electric double layer capacitance performance of porous carbons prepared by defluorination of Polytetrafluoroethylene with potassium. Electrochem. Solid-State Lett. **5**(12) (2002). https://doi.org/10.1149/1.1516909
16. O. Urper, İ. Çakmak, N. Karatepe, Fabrication of carbon nanotube transparent conductive films by vacuum filtration method. Mater. Lett. **223**, 210–214 (2018). https://doi.org/10.1016/j.matlet.2018.03.184
17. S. Zhang, Y. Li, N. Pan, Graphene based supercapacitor fabricated by vacuum filtration deposition. J. Power Sources. **206**, 476–482 (2012). https://doi.org/10.1016/j.jpowsour.2012.01.124
18. G. Kaliyaperumal, N. Padma Sravya, N. Rajendran, S. Swaminathan, V. Rathinavelu, R. Maranan, S. Sathiyamurthy, B. Haldar, Influences of electron transport layer thickness on functional characteristics of Formamidinium lead iodide featured with silver back contact solar cell. Pure Appl. Chem. (2026). https://doi.org/10.1515/pac-2025-0657
19. M.E.M. Soudagar, A. Sharma, N. Nagarajan, M. Vinayagam, S.H. Salmen, T.A. Alahmadi, Effect of electron transport layer thickness and characteristics behaviour of hybrid copper indium gallium selenide thin film solar cells. J. Power Sources. **639**(236657), 236657 (2025). https://doi.org/10.1016/j.jpowsour.2025.236657
20. N. Basavegowda, R. Chaturvedi, S. Sunitha, V. Mohanavel, K. Guruprakash, R. Venkatesh, S. Sathiyamurthy, M.E.M. Soudagar, A.H. Seikh, Influence of silver nanowire concentration on electrical and optical properties of polyaniline for transparent conductive sensors. J. Electron. Mater. **54**(9), 7232–7243 (2025). https://doi.org/10.1007/s11664-025-12174-1
21. Kim, J. H., Song, A., Park, J. M., Park, J. S., Behera, S., Cho, E., Kim, H. S. Analogous design of a microlayered silicon oxide-based electrode to the general electrode structure for thin-film lithium-ion batteries. Adv. Mater. **36**(14) (2024). https://doi.org/10.1002/adma.202309183
22. H. Xiao, X. Yang, M. Zhao, R. Zhang, Y. Jing, L. Zhang, J. Jia, Revealing promotion of interfacial Pt–O–Fe oxygen bridge structure in PtFe/graphene synthesized by a four-electrode electrochemical system on water splitting. Int. J. Hydrog. Energy. **48**(98), 38728–38741 (2023). https://doi.org/10.1016/j.ijhydene.2023.06.200
23. P. Yang, P. Wang, D. Diao, Graphene Nanosheets Enhanced Triboelectric Output Performances of PTFE Films. ACS Appl. Electron. Mater. **4**(6), 2839–2850 (2022). https://doi.org/10.1021/acsaelm.2c00334